Electronic Supplementary Material (ESI) for Journal of Materials Chemistry C.
This journal is © The Royal Society of Chemistry 2024

Electronic Supplementary Information for

In situ laser-assisted decoration of Au nanoparticles on 3D porous graphene for enhanced 2-CEES sensing

Ling Zhang, Jie Yang, Junchao Yang, Jianan Wei, Chuan Zhou, Jiang Zhao* and Qibin Huang*

State Key Laboratory of NBC Protection for Civilian, Beijing 102205, China

*Corresponding author. Email: huangqibin@sklnbcpc.cn (Q. H.) and 13021911723@163.com (J. Z.)

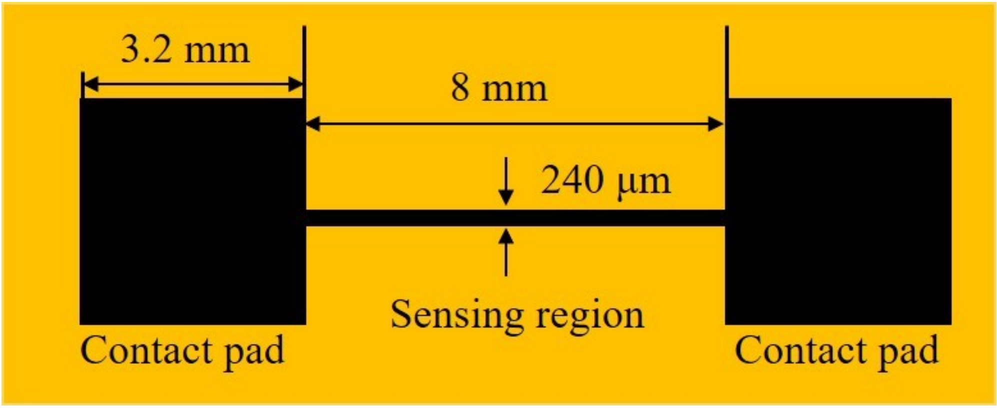

Fig. S1. Design and geometric parameters of the LIG-based gas sensor.

Fig. S2. Optical image of the flexible LIG/Au gas sensor.

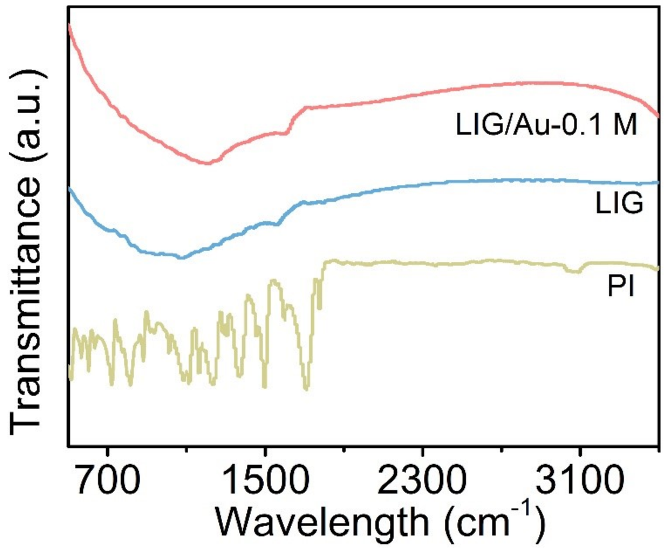

Fig. S3. FTIR spectra of PI, LIG and LIG/Au-0.1 M. FTIR spectrum of PI demonstrates that obvious peaks appear at 1090~1776 cm^{-1}, which are attributed to the stretching and bending modes of the C-O, C-N, and C=C bonds.[1] While broad absorption from 1000 cm^{-1} to 1700 cm^{-1} are both presented for LIG and LIG/Au-0.1 M, demonstrating that the laser scribing resulted in a large change in the local environment.

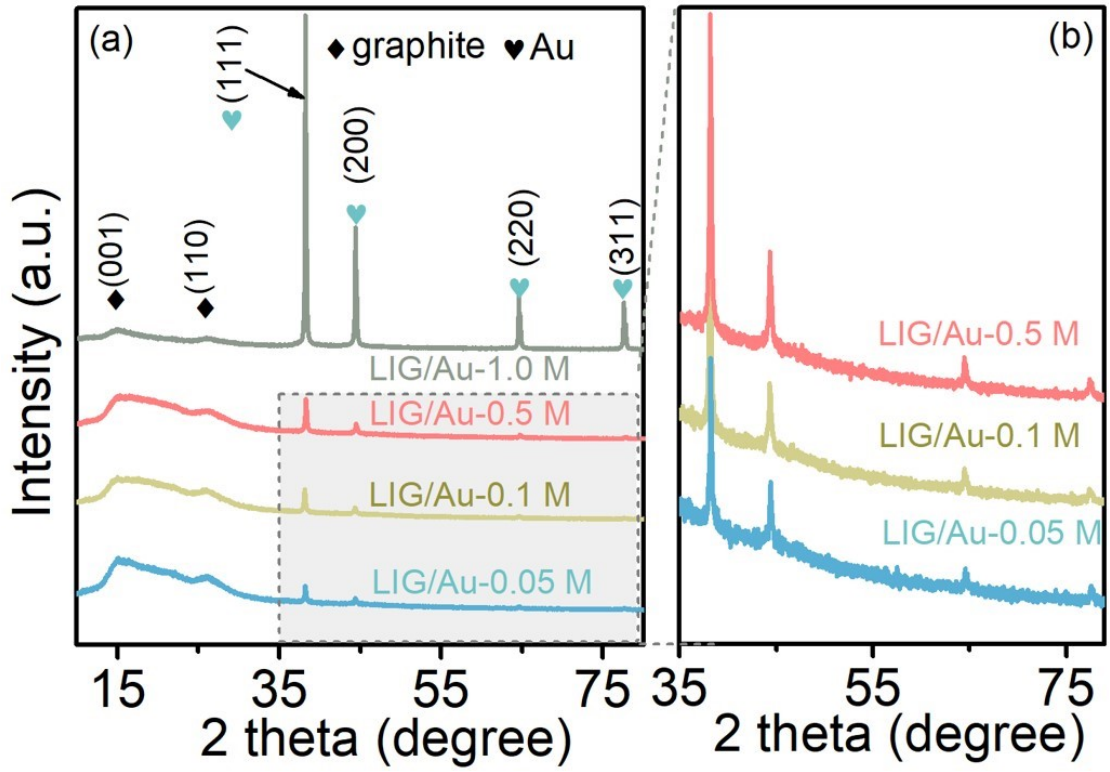

Fig. S4. (a) The XRD patterns of LIG/Au-based hybrids with various $HAuCl_4$ concentrations, and (b) Partial magnification of the XRD patterns of LIG/Au-0.05 M, LIG/Au-0.1 M and LIG/Au-0.5 M.

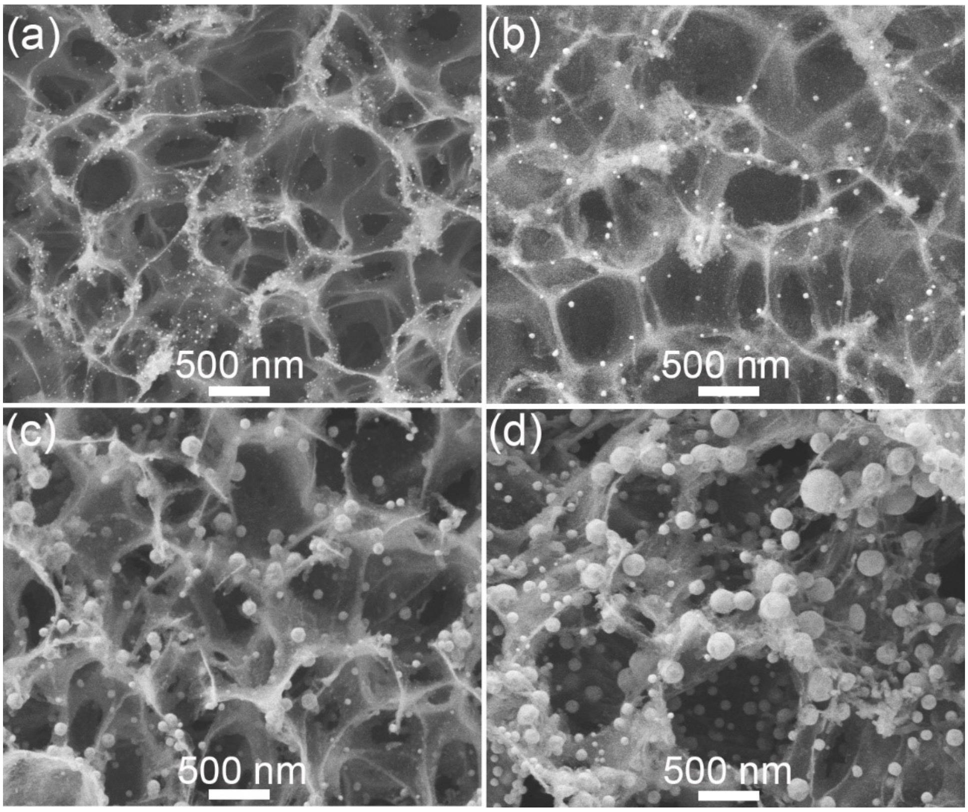

Fig. S5. (a~d) SEM images for LIG/Au-based hybrids as $HAuCl_4$ concentration varying from 0.05 to 1.0 M.

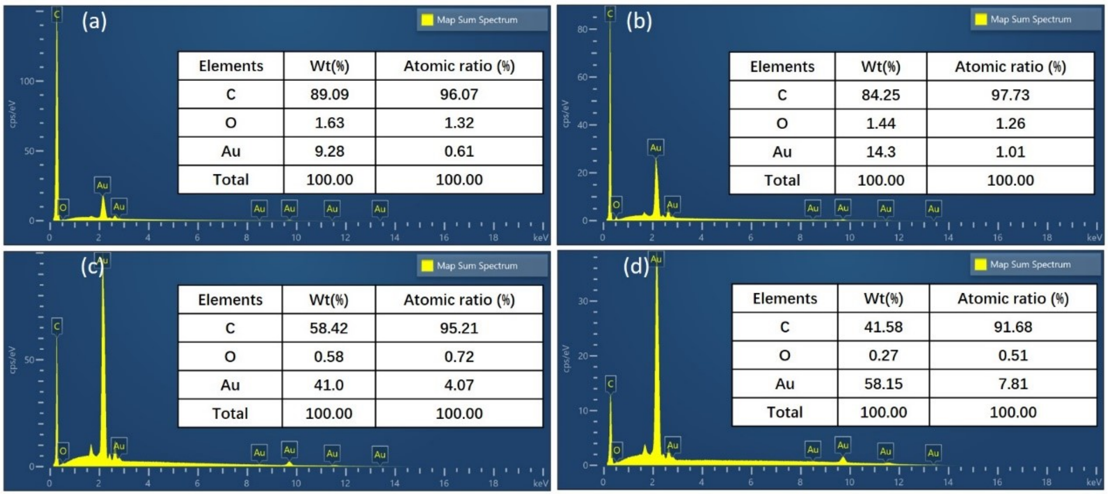

Fig. S6. (a~d) The EDX spectra of LIG/Au-0.05 M, IG/Au-0.1 M, IG/Au-0.5 M, IG/Au-1.0 M. As observed, the atomic percentage of Au increases with the increase of concentration of $HAuCl_4$.

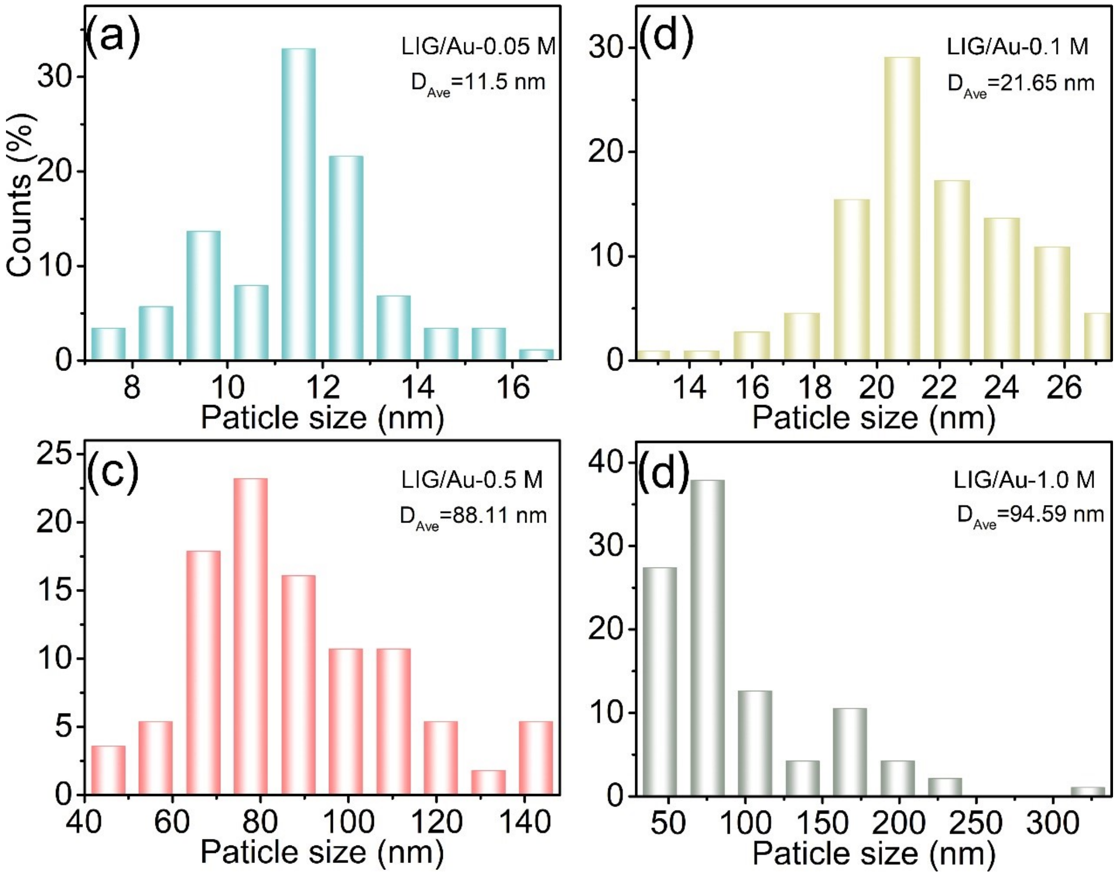

Fig. S7. Statistical distribution of particle size of Au nanoparticles in LIG/Au-0.05 M, LIG/Au-0.1 M, LIG/Au-0.5 M and LIG/Au-1.0 M.

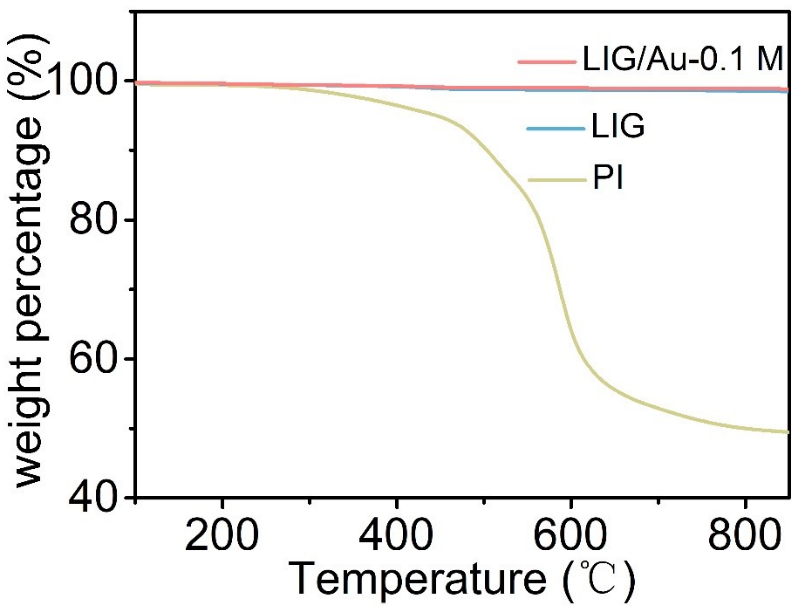

Fig. S8. Plots of TGA for PI, LIG and LIG/Au-0.1 M.

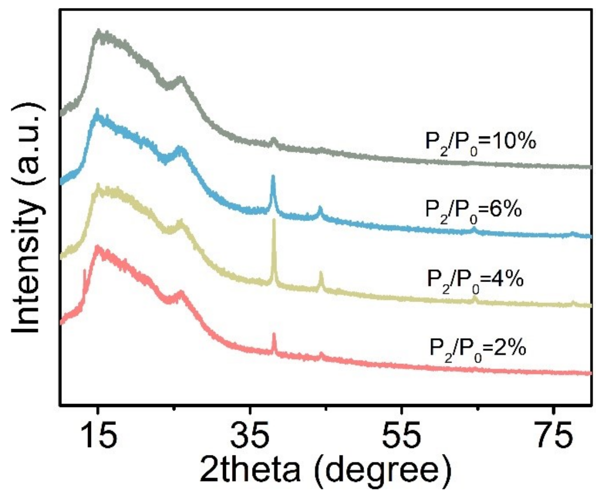

Fig. S9. The XRD patterns of LIG/Au-0.1 M hybrids fabricated under various secondary laser power (P_2/P_0=2%, 4%, 6%, 10%).

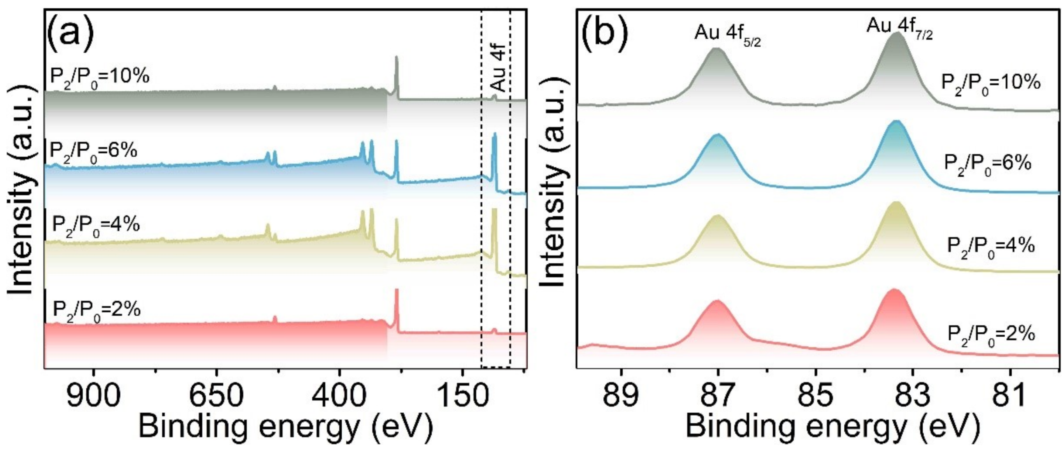

Fig. S10. (a) The wide XPS survey scans and (b) high-resolution XPS spectra of Au 4f in LIG/Au-0.1 M with different secondary laser powers (P_2/P_0=2%, 4%, 6%, 10%).

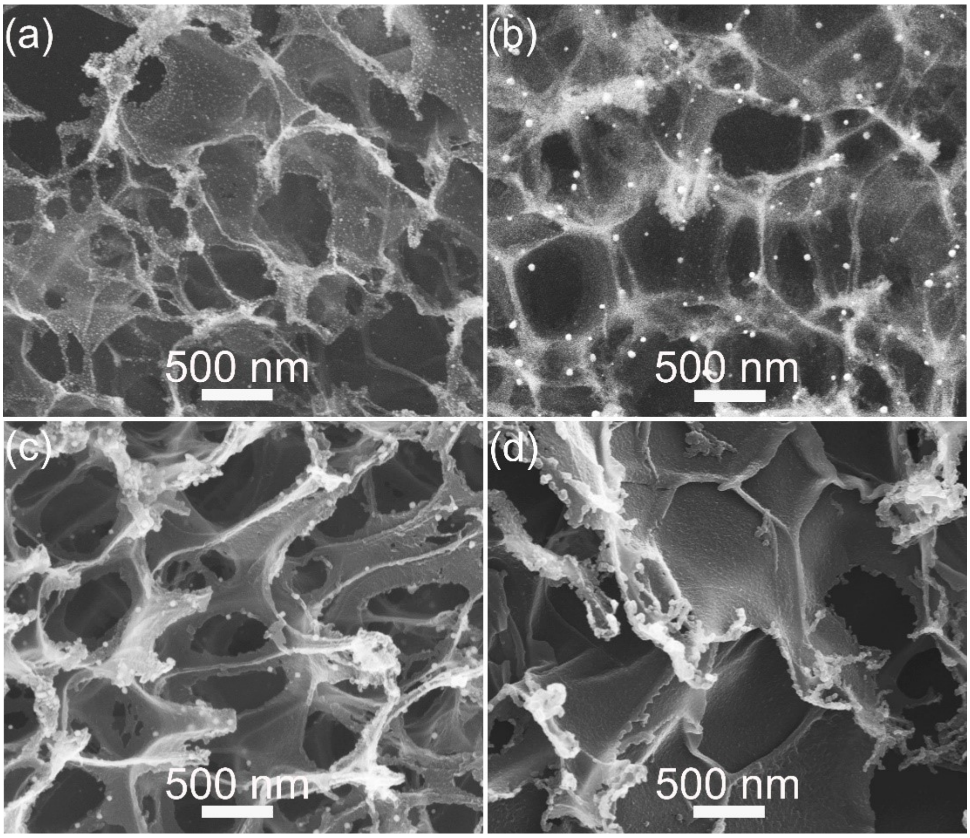

Fig. S11. (a~d) The SEM images of LIG/Au-0.1 M with different secondary laser powers (P_2/P_0=2%, 4%, 6%, 10%).

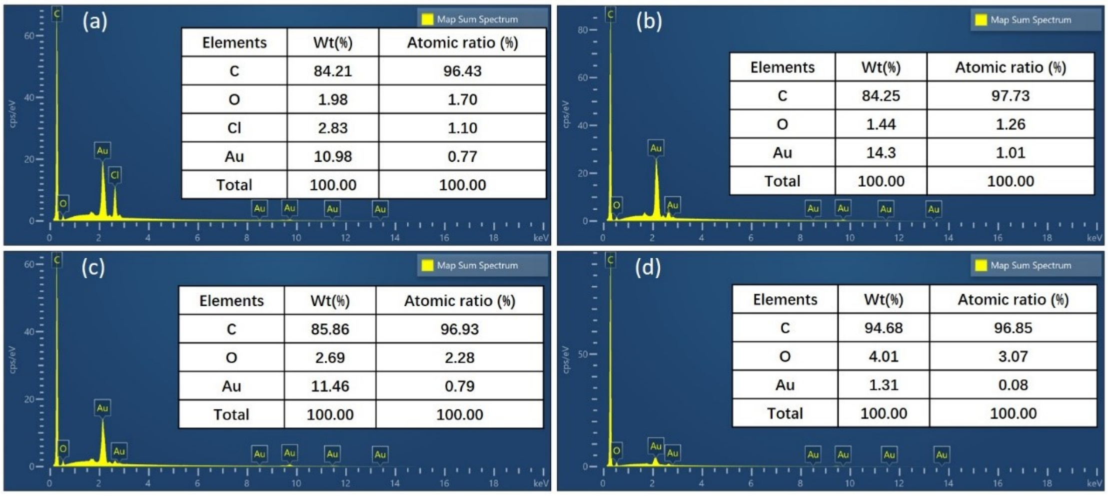

Fig. S12. (a~d) The EDX spectra of LIG/Au-0.1 M with different secondary laser power (P_2/P_0=2%, 4%, 6%, 10%). As the power increases, the atomic percentage (at%) of Au initially remains almost unchanged and then decreases. (a) The high content of Cl elemental (1.1 at%) suggests a large amount of $HAuCl_4$ had not undergone decomposition under 2%P_0. (b) Disappearance of elemental Cl and high Au content element (1.01 at%) with P_2/P_0=4% suggest the complete decomposition of $HAuCl_4$ to Au nanoparticles. (c,d) The continuous increase P_2/P_0 to 6% and 10% successively shrunk the Au content to 0.79 at% and 0.08 at%, respectively.

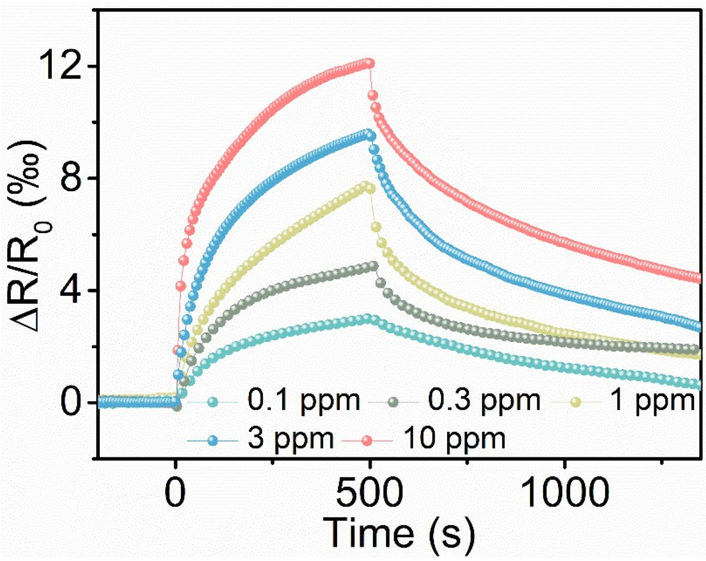

Fig. S13. Dynamic response variation upon exposure to 2-CEES with various concentrations ranging from 0.1 to 10 ppm.

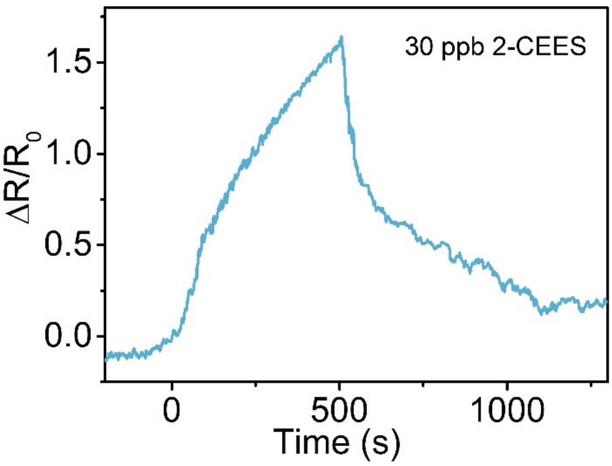

Fig. S14. Experimental demonstration of the LIG/Au-0.1 M to detect 30 ppb 2-CEES.

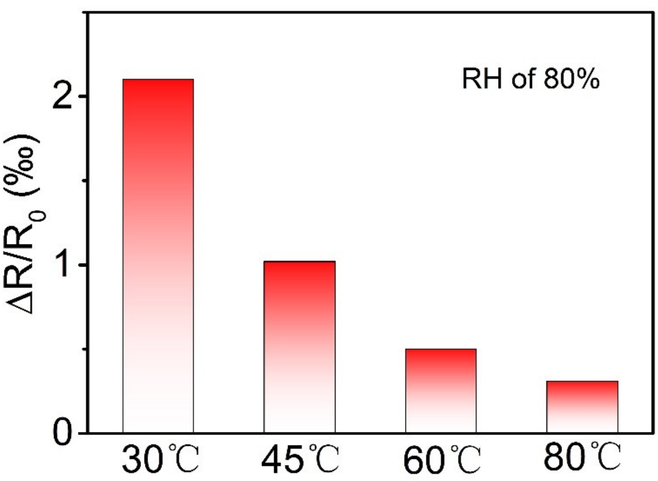

Fig. S15. Effect of the high RH of 88 % on the response of the LIG/Au-0.1 M gas sensor at temperature ranging from 30 ℃ to 80 ℃.

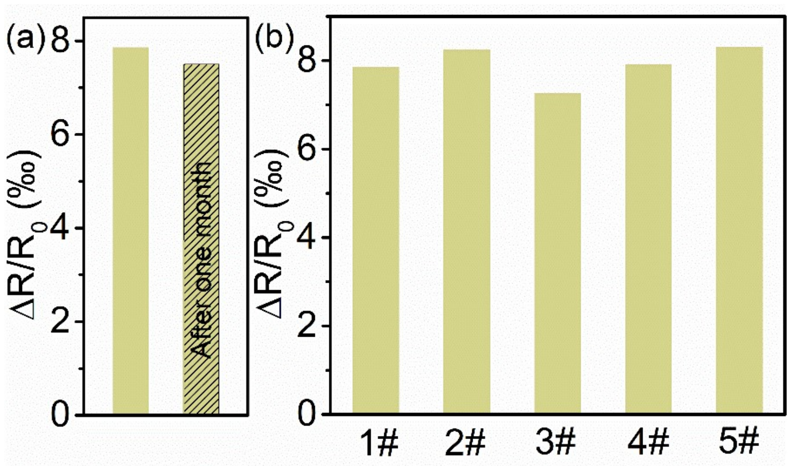

Fig. S16. (a) The responses of LIG/Au-0.1 M before and after one month. (b) The responses of five LIG/Au-0.1 M prepared under the same condition. The target gas was 1.0 ppm 2-CEES and the temperature was set as 80 °C.

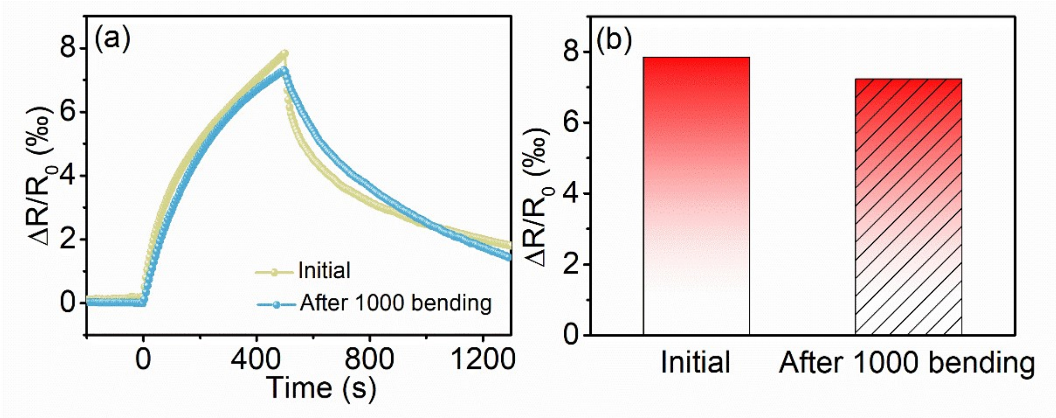

Fig. S17. The dynamic response curves of LIG/Au-0.1 M to 1.0 ppm 2-CEES at 80 ℃ before and after 1000 bending cycles with a curvature radii of 6 mm.

Table S1. Comparison of the 2-CEES sensing performances of LIG/Au-0.1 M with that in recent studies.

Material	Temperature (°C)	Range of detection (ppm)	Response /recovery time (s)	2-CEES concentration (ppm)	Sensitivity	LOD (ppb)	Selectivity	Heater	Linear range (ppm)	Ref.
Core-shell $ZnFe_2O_4$ microspheres	250	0.1~3.5	18/546	1	9.07%	＜100	YES	External heater	--	2
Al-doped ZnO NPs	500	20	--	20	954.2	--	YES	External heater	--	3
WO_3/WS_2	240	0.1~11.4	20/55	5.7	81%	＜100	YES	External heater	--	4
WO_3/graphite	260	0.1~11.4	8/34	5.7	63%	100	YES	External heater	0.1~1	5
ZnO NPs	250	0.4~20	--	1	15	400	YES	External heater	0.4~1	6
Ru-$CdSnO_3$	350	4	5/185	4	62.12	--	YES	External heater	--	7
$CdSnO_3$	350	4	2/75	4	12.05	--	YES		--	
Pt-$CdSnO_3$ thin film	300	4	8/125	4	58.63	--	YES	External heater	--	8
SnO_2-5.0 wt% Sm_2O_3	200	0.1~10	--	1	81	--	YES	External heater	--	9
LIG/Au-0.1 M	80	0.1~10	400s/--	1	7.85‰	5.8	YES	Self-heating	0.1~1	This work

References

1. J. Lin, Z. W. Peng, Y. Y. Liu, F. Ruiz-Zepeda, R. Q. Ye, E. L. G. Samuel, M. J. Yacaman, B. I. Yakobson and J. M. Tour, *Nat. Commun.*, 2014, **5**, 5714..
2. J. Yang, L. Yang, S. Cao, J. Yang, C. Yan, L. Zhang, Q. Huang and J. Zhao, *Anal. Methods*, 2023, **15**, 3084-3091.
3. R. Yoo, D. Lee, S. Cho and W. Lee, *Sens. Actuators B Chem.*, 2018, **254**, 1242-1248.
4. Y. Fan, K. Li, X. Ren, W. Yan, C. Zhu, Y. Zhao, W. Zeng, Z. Chen and S. Wang, *J. Mater. Chem. C*, 2021, **9**, 17496-17503.
5. C. Qiu, K. Li, W. Yan, Y. Fan, C. Xia, C. Sun, W. Zeng and S. Wang, *Mater. Adv.*, 2022, **3**, 6862-6868.
6. R. Yoo, C. Oh, M. J. Song, S. Cho and W. Lee, *J. Nanosci.*, 2018, **18**, 1232-1236.
7. L. A. Patil, V. V. Deo, M. D. Shinde, A. R. Bari, D. M. Patil and M. P. Kaushik, *Sens. Actuators B Chem.*, 2014, **191**, 130-136.
8. L. A. Patil, V. V. Deo, M. D. Shinde, A. R. Bari and M. P. Kaushik, *Sens. Actuators B Chem.*, 2011, **160**, 234-243.
9. H. M. Aliha, A. A. Khodadadi and Y. Mortazavi, *Sens. Actuators B Chem.*, 2013, **181**, 637-643.